IEEE Access
Multidisciplinary ⁝ Rapid Review ⁝ Open Access Journal

Received November 11, 2020, accepted December 3, 2020, date of publication December 7, 2020, date of current version December 18, 2020.

Digital Object Identifier 10.1109/ACCESS.2020.3043044

Design of a New Coded Target With Large Coding Capacity for Close–Range Photogrammetry and Research on Recognition Algorithm

JINGUI ZOU AND LIYUAN MENG, (Member, IEEE)
School of Geodesy and Geomatics, Wuhan University, Wuhan 430079, China

Corresponding author: Liyuan Meng (lymeng@whu.edu.cn)

This work was supported by the National Nature Science Foundation of China under Grant 41871373.

ABSTRACT Large-scale industrial equipment monitoring requires a large number of measurement points. To achieve fully automated measurement using photogrammetry, a large number of coded targets are required. In order to improve the coding capacity and decoding accuracy of coded targets in large-scale industrial photogrammetry, this paper designs a new coded target for digital industrial photogrammetry, which combines the characteristics of the circular coded target and the dot-distribution coded target. The max coded capacity can be 1,048,576. Experiments were carried out from different shooting angles and different distances in simple and complex scenes and the results show that the coded target is easy to be extracted and identified, with large coding capacity and high positioning accuracy. The coded target can be used for point matching and image orientation in large-scale photogrammetry, or even can be used as measuring point so as to realize the automatic management of a large number of measuring points.

INDEX TERMS Coded target, decoding, image processing, photogrammetry.

I. INTRODUCTION

Industrial close-range photogrammetry, due to its high precision and efficiency, is an ideal technical means for the installation and inspection measurement of large industrial equipment airplanes, electronic colliders, long straight rails, etc., [1]–[3]. A coded target is essential for industrial close-range photogrammetry or close-range photogrammetry in other scenes where the measured object has no obvious features [4]. A coded target can not only effectively solve the problem of the determination of corresponding points in the image matching process but improve the accuracy and precision of feature recognition as well [5].

At present, there are two mainstream kinds of coded targets, one kind is an individual target with additional, concentric patterns of material or retroreflective sheeting and the other is that of a unique and identifiable pattern of a small number of standard circular or square targets [6]–[11], as shown in Figure 1. And the mainly used two coded targets are the two in Figure 1(d) and Figure 1(h), the circular coded target and the dot-distribution coded target, respectively. The circular coded target is easy to be extracted because the recognition algorithm is relatively simple but its disadvantages are also obvious, for example, it is more susceptible

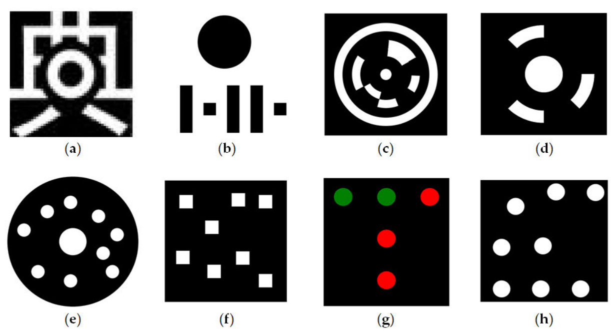

FIGURE 1. Two mainstream kinds of coded targets, (a) Y. Shi *et al.* (2020); (b) Wong *et al.* (1988); (c) NiederÖst and Maas (1997); (d) Schneider and Sinnreich(1992); (e) Sung Joon Ahn *et al.* (1999); (f) Brown and Dold (1995); (g) Cronk *et al.* (2006); (h) Hattori *et al.* (2002).

to the shooting angle than the dot-distribution coded target, which may cause misrecognition. The coding capacity of the circular coded target is small because the size of the coded bands is limited and there is no start target of the coded bands. The capacity of the circular coded target in Figure 1(d) is only 256. The dot-distribution coded target is composed of a group of regularly arranged dots, the structure of which is simple because there is only one feature. The coding capacity of the dot-distribution coded target is larger and the recognition is more stable than the circular coded target because there is a coordinate system established by some of the dots on the dot-distribution coded target, for example, the capacity of

The associate editor coordinating the review of this manuscript and approving it for publication was Geng-Ming Jiang.

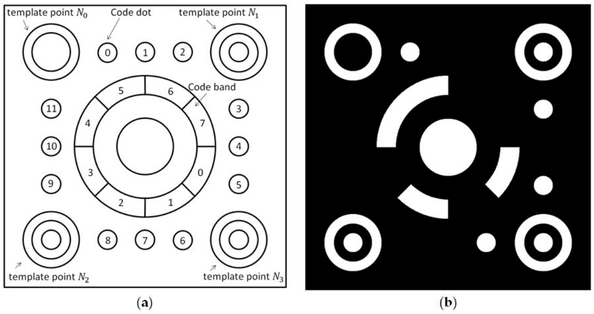

FIGURE 2. The proposed coded targets, (a) Layout of the coded target; (b) An example of the coded target.

the dot-distribution coded target in Figure 1(h) is 496. But the recognition algorithm for dot-distribution coded target is more complicated and the positioning precision of the coded target is low because the size of the location point is the same as other points and the contour center determination will be affected when the contour size is small. Due to the limitation of the coding capacity and positioning accuracy, both of the two kinds of coded targets cannot be used directly as monitoring points of large-scale industrial equipment so that automatic management of a large number of measurement points cannot be realized at present.

In order to obtain a coded target that is not only convenient to be extracted but also less affected by the shooting angle, with large coding capacity and high positioning accuracy, this paper designs a new kind of coded target composed of the circular coded target and the dot-distribution coded target. There are 4 template points, which can not only provide the start position for circular coded target to increase the coding capacity, but also can be used to calculate the projective transformation matrix to eliminate the effect of the perspective deformation, accordingly improving the accuracy of the coded target recognition. Moreover, the positioning accuracy of this code point is high and it can be directly used as the monitoring point for large industrial equipment to realize the automatic management of a large number of measurement points.

II. CODED TARGET DESIGN AND ENCODING RULES

A. CODED TARGET DESIGN

There are some principles that must be complied with when designing the coded target used in industrial close-range photogrammetry. First, the coded target must be easy to be identified because it is designed for automatic measurement. Second, the coded target should be with a sufficient coding capacity to meet the measuring needs of objects with different sizes. Third, the size of itself should not be too large, so as not to block the measuring objects. Forth, the coded target should be always different from others after translation, scaling, rotation and shear deformation so that it can help image orientation and image point matching. Fifth, it should be low production costs [12], [13].

A new kind of coded target is designed following the 5 principles above, as shown in Figure 2. Combining the circular coded target and the dot-distribution coded target, there is a 8-bit circular coded target in the middle of the coded target and the largest dot in the middle is the location dot of the circular coded target and the location dot of the new coded target as well. The dots around the circular coded target compose the dot-distribution coded target. There are four template points in the four corners. One with two concentric circles is the template point N_0 and the other three with three concentric circles each are template points called N_1, N_3 and N_2 respectively in clockwise order as shown in Figure 2(a). There are three code dots between two adjacent template points and twelve code dots in total. The coding capacity of dot-distribution coded target is 2^{12} and the total coding capacity of the new coded target is 2^{20}, which is 1,048,576 including the 8-bit circular coded target. If the circular coded target in the middle is 10-bit, the total coding capacity will be 2^{22} and the capacity will be larger when the circular coded target is with more coded bits. The calculation method of the coding capacity is shown in formula (1).

$$\text{Capacity} = 2^{n\_band+n\_codedot} \tag{1}$$

where Capacity is the coding capacity, n_band is the bit number of the circular coded target and n_codedot is the number of the code dots.

B. ENCODING RULES

As described above, the new coded target is composed of the dot-distribution coded target including 12 code dots and the 8-bit circular coded target. Correspondingly, the code is also composed of two parts, one is the dot-distribution code and the other is the circular code. For example, if the dot-distribution code is 110 and the circular code is 212, the code of the new coded target will be 110-212.

As shown in Figure 2(a), the code dots of the dot-distribution coded target are numbered clockwise from 0 to 11. When the dot color is white, the identifier will be 1 and when the dot color is black, the identifier will be 0. The dot-distribution code can be calculated using formula (2).

$$C_{dot} = \sum_{i=0}^{11} (\text{Flag}_i \cdot 2^i) \tag{2}$$

where C_{dot} is the dot-distribution code, Flag_i is the identifier of the code dot numbered i, which equals 0 or 1. In a similar way, as shown in Figure 2(a), the bit positions of the circular coded target are numbered clockwise from 0 to 7. When the bit position color is white, the identifier will be 1 and when the bit position color is black, the identifier will be 0. The circular code can be calculated using formula (3).

$$C_{circular} = \sum_{j=0}^{7} (\text{Flag}_j \cdot 2^j) \tag{3}$$

where $C_{circular}$ is the circular code, Flag_j is the identifier of the bit position numbered j, which equals 0 or 1.Since the largest number of the circular code is 255, the code of the new coded target can be calculated using formula (4) for convenience.

$$C_{new} = C_{dot} \cdot 1000 + C_{circular} \quad (4)$$

where C_{new} is the code of the new coded target.

Taking Figure 2(b) as an example, the code dots numbered 4, 5, 8 and 9 are white and according to formula (2) the dot-distribution code is 816. The bit positions on the code band numbered 1, 4, 6 and 7 are white and according to formula (3) the circular code is 210. The code of the new coded target is 816210 according to formula (4).

III. CODED TARGET RECOGNITION

Coded target recognition is the reverse process of coding the target. In this chapter, the coded target recognition algorithms and process will be described.

A. RECOGNITION ALGORITHMS

Many classical algorithms, such as binarization, contour detection, circle contour recognition and projection transformation, are used during recognition. The algorithms will be introduced in this section.

1) BINARIZATION

Image binarization is to set the gray value of pixels on the image to 0 or 255 and the purpose is to preserve the interesting part of the image maximally, which is a necessary image preprocessing process [14]. To recognize the coded target, binarization is necessary for the following code calculation and other operations. The key to binarization is the selection of the threshold. The traditional threshold selection method is to binarize the entire image with a fixed threshold, taking 127 for example, the gray value of pixels less than 127 is set to 0, and the gray value of pixels greater than or equal to 127 is set to 255. The binarization method used in this article is the maximum between-class variance method, which was proposed by Japanese scholar Otsu in 1979. It is an adaptive threshold determination method. The basic principle of the Otsu method is to find a threshold which can maximize the variance between the foreground and the background, because the variance can reflect the uniformity of the gray distribution. When the classification of the current and background is correct, the difference between the current and background parts of the image should be the biggest [15]. The binarization result of the maximum between-class variance method is shown in Figure 3 and the details are retained well. It should be noted that, in actual applications, if the illumination of the object to be measured is uneven, for example, there are shadows and variably lit areas, it is necessary to use a combination of local adaptive threshold and the Otsu method during the binarization process.

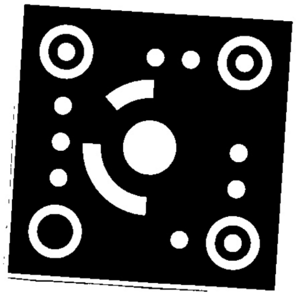

FIGURE 3. **The binarization results of the maximum between-class variance method, all elements are well distinguished.**

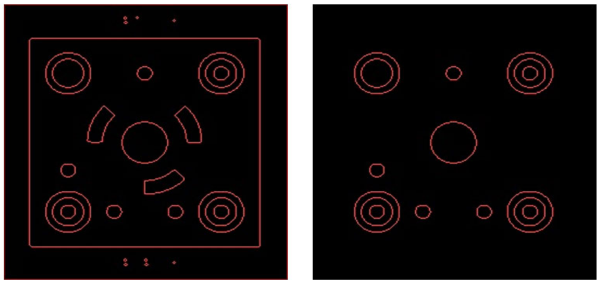

(a) (b)

FIGURE 4. **(a)The contour detection result of the Suzuki's method, (b) The circle contour recognition result, the contour detection result of the Suzuki's method the red lines are the contours detected.**

2) CONTOUR DETECTION

Contour detection is one of the fundamental techniques in the processing of images. The contour detection method used in this article is proposed by Suzuki in 1985, which derives a sequence of the coordinates or the chain codes of the contours. In the Suzuki's method, the uppermost row, the lowermost row, the leftmost column, and the rightmost column of a picture compose its frame. Pixels with gray value 0 and 1 are called the 0-pixel and the 1-pixel, respectively. A picture having the gray value f_{ij} at a the position (i, j) is expressed as $F = \{f_{ij}\}$. A 1-component and a 0-component are the connected components of 1-pixels and of 0-pixels, respectively. If a 0-component contains the frame of the picture, we call it the background; otherwise, a hole. The basic principle of the method is that if a 1-pixel having a 0-pixel in its neighborhood, it must be a contour point and the method can provide the topological relationships of the counters detected [16]. The contour detection result of the Suzuki's method is shown in Figure 4(a).

3) CIRCLE CONTOUR RECOGNITION

The template points, code dots and the location dot on the coded target are circles, so the circle contour recognition is necessary for coded target recognition. The circle contour recognition method used in this article takes advantage of a characteristic of circles that the area of the smallest circumscribed circle of a cirle should approximately equals to the area of the circle [17]. The method to find the smallest circumscribed circle is to find a circle that the points of the contour are all within the circle range and there is no cirle meeting the above condition smaller than it. The circle contour recognition result is shown in Figure 4(b).

4) PROJECTION TRANSFORMATION

The camera shooting process is the center projection process. The points on the coded target will undergo a perspective transformation. The cross ratio and the intersecting relationship of the lines will not change after a perspective

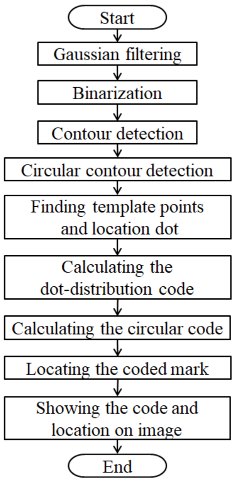

FIGURE 5. **The Coded target recognition flow, binarization, contour detection and circle contour recognition have been introduced in the previous section.**

transformation [18]. The relationship of the points before and after a perspective transformation is shown in formula (5).

$$\begin{bmatrix} x' & y' & w' \end{bmatrix} = \begin{bmatrix} u & v & w \end{bmatrix} \begin{bmatrix} a_{11} & a_{12} & a_{13} \\ a_{21} & a_{22} & a_{23} \\ a_{31} & a_{32} & a_{33} \end{bmatrix} \tag{5}$$

where u, v are the coordinates of the points before the perspective transformation and x, y are the points after the perspective transformation, where $x = x'/w'$, $y = y'/w'$. $\begin{bmatrix} a_{11} & a_{12} & a_{13} \\ a_{21} & a_{22} & a_{23} \\ a_{31} & a_{32} & a_{33} \end{bmatrix}$ is the transformation matrix, a_{11},a_{12}, a_{21}, a_{22} are the linear transformation parameters, a_{31}, a_{32} are the translation parameter and a_{13},a_{23} are the perspective transformation parameters. The transformation matrix can be calculated using 4 or more pairs of points with known corresponding coordinates according to formula (5). The coordinates of the other points after the perspective transformation can be calculated according to formula (6).

$$\begin{aligned} x &= \frac{x'}{w'} = \frac{a_{11}u + a_{21}v + a_{31}}{a_{13}u + a_{23}v + a_{33}} \\ y &= \frac{y'}{w'} = \frac{a_{12}u + a_{22}v + a_{32}}{a_{13}u + a_{23}v + a_{33}} \end{aligned} \tag{6}$$

B. CODED TARGET RECOGNITION PROCESS

The main process of recognizing the coded target proposed in this article includes Gaussian filtering, binarization, contour detection, circular contour detection, finding template points and location dot, calculating the dot-distribution code, calculating the circular code, and locating the coded target and showing the code and location on image. The overall process is shown in Figure 5. The specific process will be introduced in this section in detail.

1) FINDING THE TEMPLATE POINTS AND LOCATION DOT

There are template points, location dot and code dots on the new coded target and the template points and location dot are the main features of the new coded target. Therefore, the template points and location dot must be first recognized from the circle counters. The recognition process is shown in Figure 6. First, traverse all the circle contours and calculate the gray value of the center of each circle contour one by one. If the gray value equals 255, the circle maybe a template point of N_1, N_2 and N_3 or a non-template point. If all the gray values of the circle range equal 255, the circle is considered as a non-template point, and if the gray values change from 255, 0 to 255 from the circle center to edge, the circle is considered as a template point of N_1, N_2 and N_3 and saved to Group 1. If the gray value of the circle center equals 0 and the gray values change from 0 to 255 from the circle center to edge, the circle is considered as the template point N_0 and saved to Group 2. The location dots are found from the non-template points according to the radius relationship between the location dot and the template point.

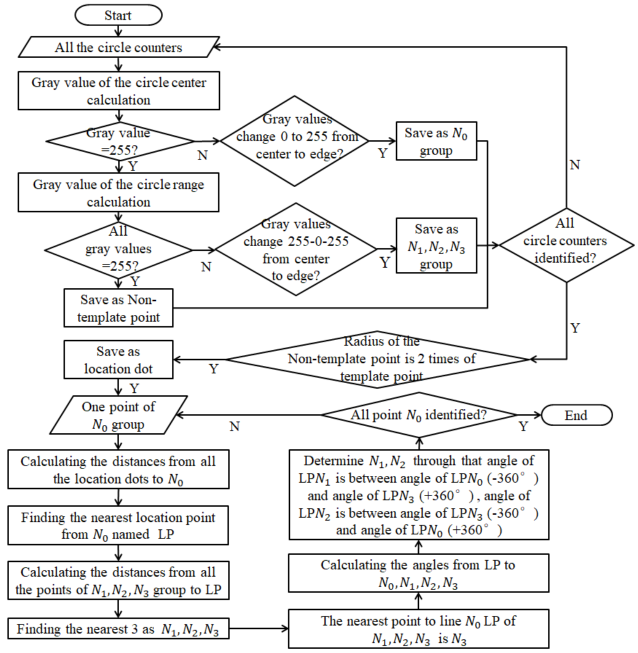

FIGURE 6. **The flow of finding and matching the template points and location dot.**

After the template points and location dots are recognized, we need to match them. Starting with the first point N_0 in Group 2, the distances from all the location dots to N_0 are calculated and we can find the nearest location point from N_0 named LP, which is considered as the location point corresponding to N_0. The distances from all the members of Group 1 to LP are calculated and we can find the nearest 3 considered as N_1, N_2 and N_3 corresponding to N_0. The one nearest to line N_0LP of N_1, N_2, N_3 is N_3 and N_1, N_2 are distinguished according to the angle relationships of the vectors from LP to each template point. The angle of the vector from LP to each template point is the angle rotating clockwise from the positive x axis to the vector and the angle value changes from 0° to 360°. When the angle of the vector in the counterclockwise direction is bigger than

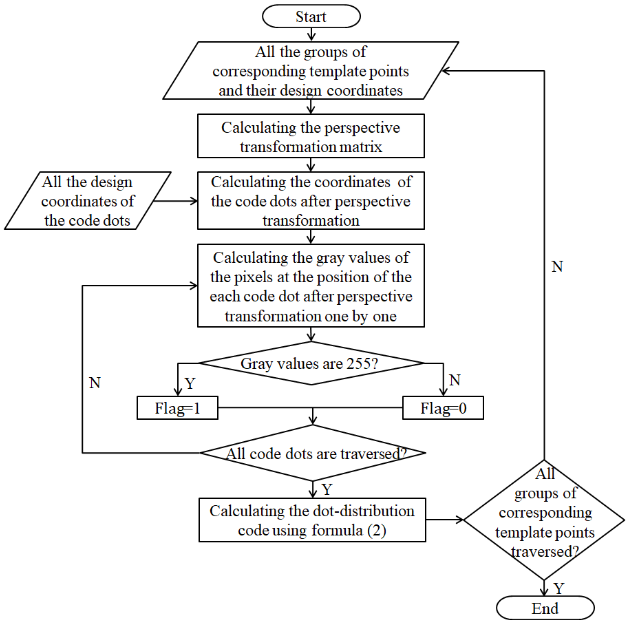

FIGURE 7. **The flow of calculating the dot-distribution code.**

that in the clockwise direction, the angle of the vector in the counterclockwise direction should be smaller by 360° or the angle of the vector in the clockwise direction should be bigger by 360°. The corresponding template points and location dots will be matched after the members in Group 2 are traversed.

2) CALCULATING THE DOT-DISTRIBUTION CODE

As introduced in subsection 3.1.4, during the shooting process the coded target will undergo a projection distortion. In order to eliminate the impact of the distortion on the code target recognition, the transformation matrix of each coded target should be calculated using the template points and the coordinates of the code dots after perspective transformation can be calculated using the transformation matrix and the design coordinates of the code dots according to formula (6). Then calculating the gray values of the pixels at the position of the each code dot after perspective transformation one by one to determine the Flag value and the dot-distribution code can be calculated using formula (2). The process is shown in Figure 7.

3) CALCULATING THE CIRCULAR CODE

The calculating of the circular codes is similar to dot-distribution codes. First the positions of the code bands after perspective transformation should be calculated and then the flag value of the each band bit can be determined. The process is shown in Figure 8. The perspective transformation of the code bands mainly causes the start and end angles' changing of each band bit. The start and end angles of each band bit are calculated using the corresponding template points and location dots, as shown in formula (7).

$$
\begin{aligned}
\mathrm{Start}_0 &= (\mathrm{Angle}_{\mathrm{LP-N_1}} + \mathrm{Angle}_{\mathrm{LP-N_3}})/2 \\
End_0 &= \mathrm{Angle}_{LP-N_3} \\
Start_1 &= \mathrm{Angle}_{LP-N_3} \\
End_1 &= (\mathrm{Angle}_{LP-N_3} + \mathrm{Angle}_{LP-N_2})/2
\end{aligned}
$$

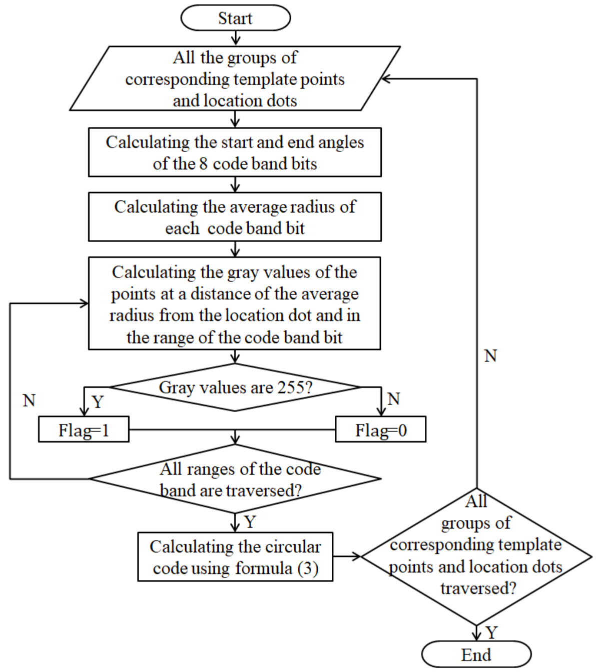

FIGURE 8. **The flow of calculating the circular code.**

$$
\begin{aligned}
Start_2 &= (\mathrm{Angle}_{LP-N_3} + \mathrm{Angle}_{LP-N_2})/2 \\
End_2 &= \mathrm{Angle}_{LP-N_2} \\
Start_3 &= \mathrm{Angle}_{LP-N_2} \\
End_3 &= (\mathrm{Angle}_{LP-N_2} + \mathrm{Angle}_{LP-N_0})/2 \\
Start_4 &= (\mathrm{Angle}_{LP-N_2} + \mathrm{Angle}_{LP-N_0})/2 \\
End_4 &= \mathrm{Angle}_{LP-N_0} \\
Start_5 &= \mathrm{Angle}_{LP-N_0} \\
End_5 &= (\mathrm{Angle}_{LP-N_0} + \mathrm{Angle}_{LP-N_1})/2 \\
Start_6 &= (\mathrm{Angle}_{LP-N_0} + \mathrm{Angle}_{LP-N_1})/2 \\
End_6 &= \mathrm{Angle}_{LP-N_1} \\
Start_7 &= \mathrm{Angle}_{LP-N_1} \\
End_7 &= (\mathrm{Angle}_{LP-N_1} + \mathrm{Angle}_{LP-N_3})/2
\end{aligned} \tag{7}
$$

where $\mathrm{Start_i}$ and $\mathrm{End_i}$ are the start and end angles of band bit i, $\mathrm{Angle_{p-q}}$ is the angle rotating clockwise from the positive x axis to the vector from point p to q and the angle value changes from 0° to 360°. When calculating the average of two angles, if one is smaller than 90° and the other is bigger than 270°, the smaller one should be bigger by 360° before the average is calculated, and when $\mathrm{Start_i}$ is bigger than $\mathrm{End_i}$, the $\mathrm{End_i}$ also should be bigger by 360°. The average radius of the code band bit is the average radius of the code band at the start and end angles.

After getting the start and end angles and the average radius of each band bit, the gray values of the points in the band bit and at a distance of the average radius from the location dot can be calculated. If the gray values are 255, the flag of the band bit is 1, otherwise it is 0. The circular code can be calculated after getting all the 8 flags of the code band bits using formula (3).

FIGURE 9. The recognition result with the ground as the background, the centers of the coded targets are targeted using red circles and the center coordinates and the codes are written on the image using blue and red respectively.

4) LOCATING THE CODED TARGET

The center of the coded target is the center of the location dot and also the middle of the four template points before perspective transformation. After perspective transformation relative position relationship among the points changes but the intersecting relationship of the lines will not change, that is, the intersection of the line N_0N_3 and line N_1N_2 is still the center of the location dot. In order to improve the positioning accuracy of the coded target, the intersection of the line N_0N_3 and line N_1N_2 is used to calculate another target center besides the center of the location dot, and the center of the coded target is determined by the average coordinates of the two centers. The center of the location dot and the four template points are determined by ellipse fitting of the contours. Because the template points are composed of two or three concentric circles, the center of each template point is determined by the average position of the centers of ellipses fitted by contours, which further improves the positioning accuracy.

IV. EXPERIMENTS AND DISCUSSION

Several experiments are designed to verify the accuracy and stability of the coded target proposed and the recognition algorithm, which are coded target recognition in different scenes, the influence of the shooting distance and angle on recognition and the effect of locating the coded target using the location pot as well as template points.

A. CODED TARGET RECOGNITION

The coded targets are shot with the ground and wall as the background, respectively. The size of the coded target used is 50mm × 50mm and the targets are placed on the ground at any rotation angle. The image resolution is 3648 × 2736. The recognition results are shown in Figure 9 and Figure 10, respectively. In the experiment all the coded targets are recognized, which shows that the coded targets and recognition algorithm proposed are available.

B. THE INFLUENCE OF THE SHOOTING DISTANCE ON RECOGNITION

The shooting distance will affect the recognition of the coded target, because it will affect the size of the coded target on the image. If the coded target on the image is too small, it cannot be recognized. The relationship of the target size and the shooting distance is shown in formula (8).

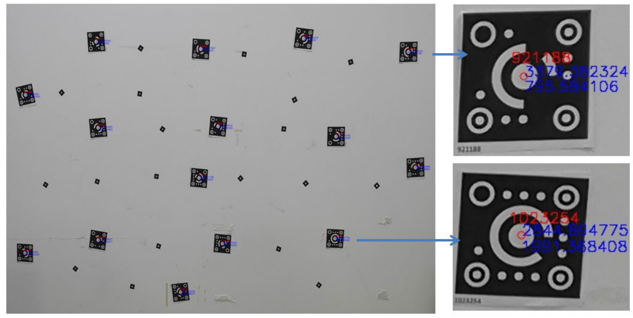

FIGURE 10. The recognition result with the wall as the background, there are other measuring dots on the image and the result is not influenced by them.

$$d = \frac{f}{S} \cdot D \tag{8}$$

where d is the side length in pixels of the coded target on the image and D is the side length of the coded target the physical world, f is the principal distance in in pixels of the camera, S is the shooting distance. According to the design parameters, when the side length of the coded target is less than 50 pixels, the radius of the template point will be less than 10 pixels, which will cause the template point to be unrecognized. In the experiment, the principal distance of the camera is 2740 pixels and the image resolution is 3648 × 2736. The coded target size is 5cm × 5cm. According to formula (8), when the shooting distance is less than 2.7m, the coded target should be recognized in theory.

In the experiments, a coded target is shot at distances of 1m, 1.5m, 2m and 2.5m, respectively and the recognition results of experiments at distances of 1m, 1.5m, 2m and 2.5m are shown in Figure 11(a), (b), (c) and (d). When the shooting distances are longer, the coded target is failed to be recognized, the main reason of which is that affected by noise, the binarization result of the template point is not ideal. It may be improved if the retro-reflective targets commonly used in industrial photogrammetry are used. Therefore, before using the proposed coded target, the longest shooting distance should be calculated using formula (8) according to the principal distance of the camera used. If a longer shooting distance is needed, the bigger size of the code target can be chosen.

C. THE INFLUENCE OF THE SHOOTING ANGLE ON RECOGNITION

The shooting angle will affect the recognition of the coded target. In order to verify the anti-photographic transformation ability of the proposed coded target, the target is shot from different angles, which are approximately 15, 30°, 45° and 60°, respectively. The recognition results are shown in Figure 12. Experiments of the shooting angles greater than 60° are also done, but the recognitions are failed because the circles distort too large to be recognized. Therefore, when

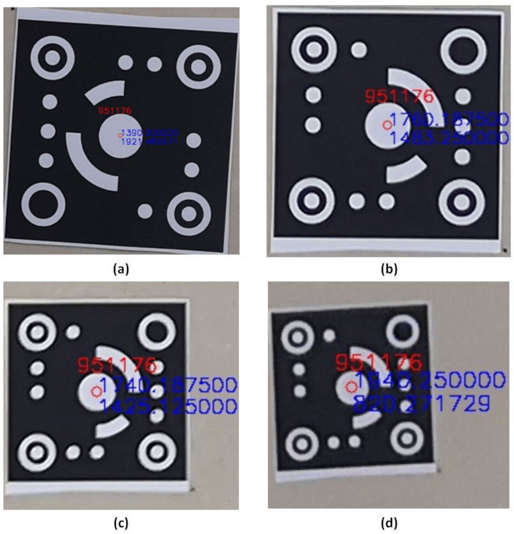

FIGURE 11. **The recognition result from different shooting distances, (a), (b), (c), (d) The results of 1m, 1.5m, 2m and 2.5m, respectively, the centers of the coded targets are targeted using red circles and the center coordinates and the codes are written on the image using blue and red respectively.**

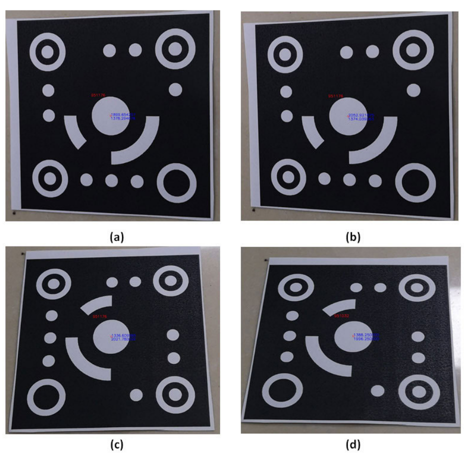

FIGURE 12. **The recognition result from different shooting angles, (a), (b), (c), (d) The results of 15°, 30°, 45° and 60°, respectively.**

using the proposed target, it should be noted that the shooting angle should be between 0° and 60°. In order to make sure that all coded targets on the image can be identified, it is best to be between 0° and 45°.

D. THE EFFECT FOR LOCATING THE CODED TARGET USING TEMPLATE POINTS

One of the characteristics of the coded target proposed is on each coded target there are four template points, which can participate in the code target's location. In order to verify the effect for locating the coded target using template points, the image of an array of coded targets are recognized and the position of each target is determined in two methods, one is using both of location dot and template points and the other is using location dot only. To eliminate the influence of distortion, the image is corrected using Zhang's calibration method before recognition. The recognized image is shown

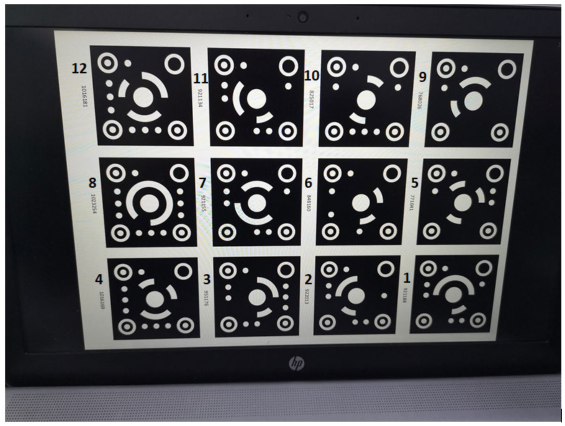

FIGURE 13. **The recognition image of the coded target array. The black numbers on the left of the coded targets are the point numbers of the centers recognized, whose coordinates are shown in Table 1.**

TABLE 1. **Coordinates of the recognized centers of the coded targets.**

	x(pixels)	y(pixels)	x'(pixels)	y'(pixels)	△x (pixels)	△y (pixels)
1	2940.17	1903.33	2940.35	1903.67	-0.18	-0.34
2	2303.11	1910.49	2303.22	1910.98	-0.11	-0.49
3	1652.63	1921.14	1652.87	1921.28	-0.24	-0.14
4	982.86	1931.69	982.921	1931.98	-0.061	-0.29
5	3001.94	1300.06	3001.88	1300.12	0.06	-0.06
6	2333	1300.75	2333	1300.5	0	0.25
7	1651.28	1303	1651.56	1303	-0.28	0
8	947.202	1304.03	947.404	1304.06	-0.202	-0.03
9	3071.04	633.448	3071.07	633.896	-0.03	-0.448
10	2368.25	626.75	2368.5	627.5	-0.25	-0.75
11	1649.27	619.304	1649.54	619.608	-0.27	-0.304
12	905.362	609.329	905.724	609.659	-0.362	-0.33

in Figure 13 and the black numbers on the left of the coded targets are the point numbers of the centers recognized. The coordinates of the recognized centers of the coded targets are listed in Table 1. The second and third columns are the coordinates using both of location dot and template points, and the forth and the fifth columns are the coordinates using location dot only. The last two columns are the differences of the two kinds of coordinates.

Although there is a perspective transformation, the points in a line are still in a line after the perspective transformation. The positioning accuracy of the two methods can be evaluated using the property by contrasting the straight line deviation of the points which are designed in a line. The process of calculating the straight line deviation is first calculating the equation of the line from the start point to the end point, which is named baseline, and then calculating the average distance from the other points designed to be in a line with the start and end points to the baseline. In this experiment, there are seven lines formed from the coded target centers and the straight line deviations are shown in Table 2. The start and end point of the lines are shown in the second and third columns corresponding to Figure 13. The forth and the fifth columns are the straight line deviations using both of location dot and template points and using location dot only, respectively. The last column is the differences of the straight line deviations in two coded target location methods.

TABLE 2. Straight line deviation comparing using template points or not.

Line	Start point	End point	Straight line deviation d (pixels)	Straight line deviation d' (pixels)	△d (pixels)
1	4	1	1.46	1.46	0
2	8	5	0.47	0.6	-0.13
3	12	9	1.41	1.54	-0.13
4	12	4	0.4	0.6	-0.2
5	11	3	1.04	1.26	-0.22
6	10	2	0.24	0.27	-0.03
7	9	1	1.12	1.14	-0.02

As can be seen from the Table 2, six of the seven straight line deviations' accuracy increases after adding template points in calculating the center coordinates and the Line 5 improves most by 0.22 pixels, which illustrates that the positioning accuracy of the coded targets can be improved to a certain extent using the template points.

V. CONCLUSION

A new coded target for digital industrial photogrammetry is designed, which combines the characteristics of the circular coded target and the dot-distribution coded target and there are template points on the coded target. The recognition algorithms are studied on, such as binarization, contour detection, circle contour recognition and projection transformation, and the recognition of the new coded target is realized. Experiments show that the new coded target can be recognized at shooting angles between 0° and 60° and the positioning accuracy of the coded targets can be improved using the template points.

The new coded target increases the coding capacity of the existing coded targets and improves the positioning accuracy of the coded targets, providing a new choice of the coded target in the industrial chose-range photogrammetry. But it can be improved in some aspects, for example, a better ellipse detection algorithm can be used to improve the recognition success rate from a larger angle and other positioning algorithms, like gray-weighted centroid method can be used to improve the positioning accuracy further. In the future, combining with the database management technology, the automatic management of a large number of measuring points in large-scale photogrammetry will be realized using the proposed coded target.

REFERENCES

[1] T. Luhmann, "Close range photogrammetry for industrial applications," *ISPRS J. Photogramm. Remote Sens.*, vol. 65, no. 6, pp. 558–569, Nov. 2010, doi: 10.1016/j.isprsjprs.2010.06.003.

[2] I. Goda, G. L'Hostis, and P. Guerlain, "*In-situ* non-contact 3D optical deformation measurement of large capacity composite tank based on close-range photogrammetry," *Opt. Lasers Eng.*, vol. 119, pp. 37–55, Aug. 2019, doi: 10.1016/j.optlaseng.2019.02.006.

[3] L. Jing, D. Lan, W. Tong, Z. Hongyan, and W. Xiaolong, "Application of close-range photogrammetry to particle accelerator alignment," *High Power Laser Part. Beams*, vol. 31, no. 3, pp. 73–77, 2019, doi: 10.11884/HPLPB201931.180333.

[4] G. P. Huang, *The Theory, Method and Application of Digital Close-Range Industrial Photogrammetry*, 1st ed. Beijing, China: Science Press, 2016, pp. 122–130.

[5] C. S. Fraser, "Innovations in automation for vision metrology systems," *Photogramm. Rec.*, vol. 15, no. 90, pp. 901–911, Oct. 1997.

[6] Y. Shi and L. Zhang, "Design of chinese character coded targets for feature point recognition under motion-blur effect," *IEEE Access*, vol. 8, pp. 124467–124475, 2020.

[7] K. Forbes, A. Vougt, and N. Bodika, "An inexpensive, automatic and accurate camera calibration method," *Proc. 13th Annu. South Afr. Workshop Pattern Recognit.*, 2002, pp. 1–6.

[8] S. J. Ahn, W. Rauh, and S. I. Kim, "Circular coded target for automation of optical 3d-measurement and camera calibration," *Int. J. Pattern Recognit. Artif. Intell.*, vol. 15, no. 6, pp. 905–919, Sep. 2001, doi: 10.1142/S0218001401001222.

[9] S. Hattori, K. Akimoto, C. Fraser, and H. Imoto, "Automated procedures with coded targets in industrial vision metrology," *Photogramm. Eng. Remote Sens.*, vol. 68, no. 5, pp. 441–446, 2002.

[10] R. Chen, K. Zhong, Z. Li, and M. Liu, "An accurate and reliable circular coded target detection algorithm for vision measurement," *Proc. SPIE*, vol. 10023, Nov. 2016, Art. no. 1002319, doi: 10.1117/12.2245590.

[11] M. R. Shortis and J. W. Seager, "A practical target recognition system for close range photogrammetry," *Photogramm. Rec.*, vol. 29, no. 147, pp. 337–355, Sep. 2014. 10.1111/phor.12070.

[12] T. Luhmann, *Close-Range Photogrammetry and 3D Imaging*, 2nd ed. Berlin, Germany: De Gruyter, 2014, pp. 230–231.

[13] Q. Feng, Z. Li, and G. Li, "Design and decoding of dot-distribution coded targets," in *Proc. 8th World Congr. Intell. Control Autom.*, Shandong, China, Jul. 2010, pp. 5381–5384.

[14] Y. H. Jia, *Digital Image Processing*. 1st ed. Wuhan, China: Wuhan Univ. Press, 2015, pp. 155–157.

[15] N. Otsu, "A threshold selection method from gray-level histograms," *IEEE Trans. Syst., Man, Cybern.*, vol. SMC-9, no. 1, pp. 62–66, Jan. 1979, doi: 10.1109/TSMC.1979.4310076.

[16] S. Suzuki and K. Be, "Topological structural analysis of digitized binary images by border following," *Comput. Vis., Graph., Image Process.*, vol. 30, no. 1, pp. 32–46, Apr. 1985, doi: 10.1016/0734-189X(85)90016-7.

[17] B. Gary and K. Adrian, *Learning Open CV*. Newton, MA, USA: O'Reilly Media, 2009, pp. 222–262.

[18] R. Hartley and A. Zisserman, *Multiple View Geometry in Computer Vision*, 2nd ed. Cambridge, U.K.: Cambridge Univ. Press, 2004, pp. 32–51.

JINGUI ZOU was born in Hubei, China, in 1972. He received the B.S. and Ph.D. degrees in geodesy and geomatics from Wuhan University, Wuhan, in 2002.

Since 2010, he has been a Professor with the School of Geodesy and Geomatics, Wuhan University. He is the author of more than 100 articles. His research interests include precision engineering survey, deformation monitoring, and multi-source technology fusion.

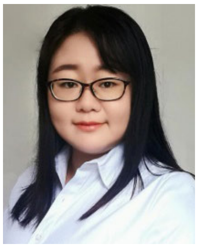

LIYUAN MENG (Member, IEEE) received the B.S. degree in geodesy and geomatics from Wuhan University, Wuhan, China, in 2011, and the M.S. degree in photogrammetry and remote sensing from the Hefei University of Technology, Hefei, in 2015. She is currently pursuing the Ph.D. degree in geodesy and geomatics with Wuhan University.

Her research interests include the image processing, close-range photogrammetry, and precision Engineering Survey.